

Quantum simulation and quantum computation of noisy-intermediate scale

Kai Xu(许凯) and Heng Fan(范桁)

Citation: Chin. Phys. B, 2022, 31 (**10**): 100304. DOI: 10.1088/1674-1056/ac89de
Journal homepage: http://cpb.iphy.ac.cn; http://iopscience.iop.org/cpb

What follows is a list of articles you may be interested in

Direct measurement of two-qubit phononic entangled states via optomechanical interactions

A-Peng Liu(刘阿鹏), Liu-Yong Cheng(程留永), Qi Guo(郭奇), Shi-Lei Su(苏石磊), Hong-Fu Wang(王洪福), and Shou Zhang(张寿)

Chin. Phys. B, 2022, 31 (**8**): 080307. DOI: 10.1088/1674-1056/ac5d2f

Analysis and improvement of verifiable blind quantum computation

Min Xiao(肖敏) and Yannan Zhang(张艳南)

Chin. Phys. B, 2022, 31 (**5**): 050305. DOI: 10.1088/1674-1056/ac2f34

Beating standard quantum limit via two-axis magnetic susceptibility measurement

Zheng-An Wang(王正安), Yi Peng(彭益), Dapeng Yu(俞大鹏), and Heng Fan(范桁)

Chin. Phys. B, 2022, 31 (**4**): 040309. DOI: 10.1088/1674-1056/ac4229

Low-overhead fault-tolerant error correction scheme based on quantum stabilizer codes

Xiu-Bo Chen(陈秀波), Li-Yun Zhao(赵立云), Gang Xu(徐刚), Xing-Bo Pan(潘兴博), Si-Yi Chen(陈思怡), Zhen-Wen Cheng(程振文), and Yi-Xian Yang(杨义先)

Chin. Phys. B, 2022, 31 (**4**): 040305. DOI: 10.1088/1674-1056/ac3817

Quantum simulation of lattice gauge theories on superconducting circuits: Quantum phase transition and quench dynamics

Zi-Yong Ge(葛自勇), Rui-Zhen Huang(黄瑞珍), Zi-Yang Meng(孟子杨), and Heng Fan(范桁)

Chin. Phys. B, 2022, 31 (**2**): 020304. DOI: 10.1088/1674-1056/ac380e

---

TOPICAL REVIEW — Celebrating 30 Years of *Chinese Physics B*

Quantum simulation and quantum computation of noisy-intermediate scale

Kai Xu(许凯)[1,2,3,4,5,†] and Heng Fan(范桁)[1,2,3,4,5,‡]

[1] *Beijing National Laboratory for Condensed Matter Physics, Institute of Physics, Chinese Academy of Sciences, Beijing* 100190, *China*
[2] *Beijing Academy of Quantum Information Sciences, Beijing* 100190, *China*
[3] *School of Physical Sciences, University of Chinese Academy of Sciences, Beijing* 100190, *China*
[4] *CAS Center of Excellence in Topological Quantum Computation, University of Chinese Academy of Sciences, Beijing* 100190, *China*
[5] *Songshan Lake Materials Laboratory, Dongguan* 523808, *China*

(Received 13 June 2022; revised manuscript received 12 August 2022; accepted manuscript online 16 August 2022)

In the past years, great progresses have been made on quantum computation and quantum simulation. Increasing the number of qubits in the quantum processors is expected to be one of the main motivations in the next years, while noises in manipulation of quantum states may still be inevitable even the precision will improve. For research in this direction, it is necessary to review the available results about noisy multiqubit quantum computation and quantum simulation. The review focuses on multiqubit state generations, quantum computational advantage, and simulating physics of quantum many-body systems. Perspectives of near term noisy intermediate-quantum processors will be discussed.

Keywords: quantum computation, quantum simulation, many-body physics, quantum supremacy, noisy intermediate-scale quantum technologies

PACS: 03.67.–a, 03.67.Bg, 03.67.Lx **DOI:** 10.1088/1674-1056/ac89de

1. Introduction

Quantum computation may surpass the current computers, exponentially or polynomially, by performing specific quantum algorithms. Quantum simulation can emulate, in a controllable way, the quantum phenomena which happen in the world from micro-scale to the universe. A prerequisite for practical useful quantum computation and quantum simulation is that the number of qubits of the quantum processor should be larger than a value, such that the performed tasks are beyond the computational capability of current available computers. Recently, a series of results by using multiqubit quantum processors have been presented. The number of coherently controlled qubits ranges from several to dozens of qubits, and may achieve around 100 in the near future. In contrast with previous results, there are some new characteristics about those developments: (i) Simulations and computations are for general schemes, which are less about the physics or mechanism of the processors themselves, but may be realizable in different platforms. (ii) Controlling complexities and data sets of experiments grow in general exponentially with the number of qubits, which need advanced integration and high efficiency of the platforms. (iii) Decoherence, inaccurate controlling and readout limit the precision of the results and the schemes chosen. The performed schemes in general should not involve large depth of circuits because of limited accuracy of the controlling, and should avoid long time evolution due to limited coherence time. Those characteristics are described as noisy intermediate-scale quantum (NISQ) technologies.[1]

Remarkably, by increasing the number of qubits and improving control precision, the noisy multiqubit quantum computation and quantum information recently achieve the aim of quantum supremacy,[2,3] i.e., surpassing the computational capability of any current computers for specific tasks. The next stages may be the quantum advantage, implying practical useful quantum information processing, and universal quantum computation and quantum simulation, still assistance of classical digital processors may be necessary. We remark that there is no clear distinction between quantum supremacy and quantum advantage.

Although the near-term noisy multiqubit quantum processors may not be practical useful for our everyday life, researchers are optimistic about the applications for a prototype of quantum computer (see Fig. 1). The applications under consideration include, but not limited to, simulation of quantum many-body physics,[4–8] simulation of quantum chemistry,[9] hybrid classical and quantum processors with task assignment,[10] quantum machine learning and quantum artificial intelligence.[11–13] Indeed, great progresses have been made in those directions. Here, we would like to review those results, to summarize what have been achieved, at the same time, to expect aims for future research.

The concept of a universal quantum simulator was pro-

†Corresponding author. E-mail: kaixu@iphy.ac.cn
‡Corresponding author. E-mail: hfan@iphy.ac.cn

© 2022 Chinese Physical Society and IOP Publishing Ltd

posed by Feynman,[14] with which various quantum phenomena can be simulated using a controllable quantum machine. This machine then can also perform universal quantum computing since the general unitary transformation can be implemented. In this sense, the universal quantum simulator and quantum computer are equivalent, while one emphasizes to reproduce quantum phenomena in an analogous way, another is concerning about the realization of computing tasks. A universal quantum simulator can be implemented by an analog method, implying the Hamiltonian is realized by a similar Hamiltonian, or a digital method by decomposing the evolution into logical gates of a universal set of quantum computation.

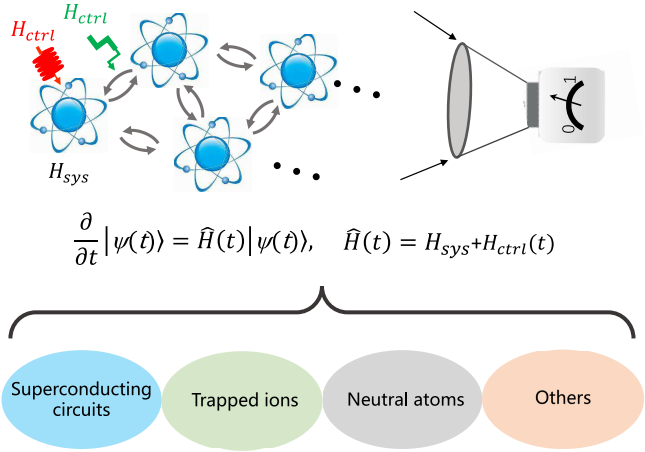


Fig. 1. Controllable quantum systems for quantum computing and simulation. To realize a quantum simulator or a quantum computer, the system often contains lots of natural atoms or artificial atoms and have couplings between the atoms. The system Hamiltonian can be divided into two parts: the static part $H_{\rm sys}$ which stays fixed after sample fabrication and the dynamic controllable part $H_{\rm ctrl}$ which can be regulated through applying external signals. State evolution can then be steered through adjusting $H_{\rm ctrl}$ according to the Schrödinger equation. Promising physical candidates include superconducting circuits, trapped ions, neutral atoms, and so on.

Quantum simulations of many-body system are appealing with noisy multiqubit quantum processors, in particular in studying dynamical properties. In general, the simulation scheme can be as follows: Preparation of an initial state which can be a product state or entangled state from a product state by simple operations, or a state which can be easily obtained for the quantum simulators. Next, the initial state can be manipulated by operations or evolves according to controllable Hamiltonian. Then, the intermediate or final state will be read out by measurement. There are some reasons that the many-body simulations are very useful at the present stage. (i) The physics such as phases of quantum many-body system may be robust such that the characteristic phenomena can be demonstrated properly with noisy multiqubit quantum processor, arbitrary accuracy may not be necessary even improving precision is plausible. (ii) The condensed matter physics of many-body system have been well studied, the complexity or extent of the complication of the problems is generally known. In this sense, the motivation of simulation can aim to solving open or hard problems. (iii) For superconducting qubits or other simulators, the devices of qubits can be designed based on different models with configurations for qubit locations like one-dimension, square lattice, honeycomb, Kagome, etc. Different Hamiltonian can be realized based on the specifically designed hardware or platforms.

The simulation of quantum chemistry is promising since the practical applications may range in many fields like drug synthesis, biological nitrogen fixation, etc.[9] The main problem is the necessity for high precision in simulation. However, some tasks may concern more about the speed of computation and simulation, for which the near-term quantum simulation may still possess advantageous.

2. Simulation of many-body physics using trapped ions and Rydberg atoms

Trapped ions and Rydberg atoms are promising physical candidates for implementing quantum simulation.[15,16] Recently, the number of qubits for quantum simulators reaches 51 with neutral cold ^{87}Rb Rydberg atoms,[4] and 53 for trapped ions.[5] Dynamics of many-body physics can be studied by those simulators.

For the system with Rydberg atoms, the Hamiltonian is written as[4]

$$\frac{\mathcal{H}}{\hbar} = \sum_{i<j} V_{ij} n_i n_j + \sum_i \frac{\Omega_i}{2} \sigma_x^i - \sum_i \Delta_i n_i, \tag{1}$$

where Pauli matrix, $\sigma_x^i = |g_i\rangle\langle r_i| + |r_i\rangle\langle g_i|$, is defined as the coupling between the ground state $|g_i\rangle$ and the Rydberg state $|r_i\rangle$ of an atom at site i, and is driven at Rabi frequency Ω_i. The driving lasers detunings from the Rydberg state are Δ_i, and $n_i = |r_i\rangle\langle r_i|$. The qubit–qubit interactions V_{ij} are due to van der Waals interactions between pairs of Rydberg atoms depending on their distances R_{ij}, $V_{ij} = C/R_{ij}^6$, where $C > 0$ is the repulsive van der Waals coefficient.

This system is a quantum many-body Ising spin model. For homogeneous case, $|\Omega_i| = \Omega, \Delta_i = \Delta$, which is realized by aligning the beams to globally address all trapped atoms with a uniform Rabi frequency and the same detunings. The parameters $\Omega(t)$ and $\Delta(t)$ are controlled by changing the laser intensities and detunings in time. The strengths of interactions V_{ij} are controlled by varying the distances between the atoms or coupling to a different Rydberg state. The Rydberg–Rydberg interactions V_{ij} will prevent nearby atoms from simultaneous excitations into Rydberg states due to the Rydberg blockade mechanism. Individual atoms are trapped using optical tweezer arrays, which are created by an acousto-optical deflector. The Rydberg atoms are arrayed in one-dimensional lattice thus with power law decay interactions $1/|i-j|^6$ with distance for V_{ij}.

The experiments start with loading the atoms into the tweezer arrays, which are defect-free after procedures like fluorescence imaging and rearrangements. The initial state then can be prepared as a product state with all atoms in the ground state $|g_1...g_N\rangle$ by optical pumping. The traps are then turned off (the interaction between the atoms and tweezer arrays become repulsive when the atoms are in excited states, which will cause a serious atom loss if it is not turned off), and the driving lasers are switched on with controlled pulse $\Omega(t)$ and detuning $\Delta(t)$. The system will evolve under the unitary time evolution governed by Hamiltonian (1). The final states can be readout by turning the traps back on and imaging the atomic fluorescence. The ground state $|g\rangle$ atoms can be imaged, while the Rydberg state $|r\rangle$ atoms will be ejected with absence of fluorescence. In the period of evolution without traps, the atomic motion away from the trapping region limits the time of coherence. Within 4 μs period of time evolution, the atomic loss probability is about 0.1%, and around 2% at 6 μs, with temperature 12 μK. To limit the infidelity with 3%, the experiments operate with trap-off time of ≤ 7 μs.

For resonant driving $\Delta = 0$ and far spatially separated atoms without interaction, Rabi oscillations happen between ground state $|g\rangle$ and Rydberg state $|r\rangle$ for a single atom. The amplitude of the Rabi oscillations is limited by the detection probabilities of the states, $f_r = 0.93, f_g = 0.98$, denoting the probabilities to correctly detect states, $|r\rangle$ and $|g\rangle$, respectively. When the atoms are close to each other with distance $a < R_\mathrm{b}$, where R_b defines the Rydberg blockade radius, the Rabi oscillations happen between the ground state and a collective superposed state with one excitation, $|W\rangle = \frac{1}{\sqrt{N}}\sum_j |g_1...r_j...g_N\rangle$, here the collective Rabi frequency scales as $\sqrt{N}$.

States of Rydberg crystals break distinct spatial symmetries for different quantum phases. By using quantum simulator of Rydberg atoms, antiferromagnetic ordered states with $\mathbb{Z}_2$, $\mathbb{Z}_3$ and $\mathbb{Z}_4$ broken symmetries have been prepared experimentally in an Ising-type quantum chain with couplings decaying fast over distance between atoms.[4] The $\mathbb{Z}_2$ order state breaks translational symmetry and corresponds to antiferromagnetic state $|rgr\cdots rgr\rangle$. In experiment, all atoms are prepared initially in the ground state by optical pumping, $|g\cdots g\rangle$. The detunings of the driving lasers are controlled so that Δ/Ω sweeps adiabatically from large negative values to large positive values. For large negative values Δ/Ω, the ground state corresponds to the initial state $|g\cdots g\rangle$. As Δ/Ω increases slowly from negative values to positive values, the number of Rydberg excitations $|r\rangle$ increases and their interactions become important. With appropriate distance between atoms, the Rydberg blockade is effective for nearest-neighbor atoms, but with negligible next-nearest-neighbor interactions $V_{j,j+2}$, resulting in Rydberg excitation occurs at every other atom, in the form $|rgrgrg\cdots rgr\rangle$. In this case, the $\mathbb{Z}_2$ order state is obtained.

The $\mathbb{Z}_3$ and $\mathbb{Z}_4$ order states take the forms of $|rggr\cdots rggr\rangle$ and $|rgggr\cdots rgggr\rangle$, respectively. Similar to the $\mathbb{Z}_2$ order state preparation, by reducing the distances between atoms, more atoms may lie within Rydberg blockade radius and thus they are prevented from excitation, corresponding non-negligible next-nearest-neighbor interactions. The resulting state takes the from $|rggrggr\cdots rggr\rangle$. Then, the $\mathbb{Z}_3$ order state can be obtained. And reducing further the spacing between atoms, one can obtain the $\mathbb{Z}_4$ order state.

In trapped-ion system presented in Ref. [5], the Hamiltonian is written as the transverse-field Ising model

$$H = \sum_{i<j} J_{ij}\sigma_i^x\sigma_j^x + B_z\sum_i \sigma_i^z, \tag{2}$$

where the couplings induced by the applied laser field take approximately as $J_{ij} \approx J_0/|i-j|^\alpha$, i, j are sites for a chain of up to 53 ions, power exponent α is set between 0.8 to 1. The transverse field is adjusted by a controllable Stark shift from the laser field.

The dynamics of the system from an initial state can then be studied. The magnetization of each spin $\langle\sigma_i^x\rangle$ can be measured by site-resolved fluorescence, with the help of qubits rotation. The detection efficiency of the spin qubit is about 99%. Dynamics of quantum quench for different cases determined by ratio of transverse field and Ising coupling are experimentally studied. The time-dependent magnetization shows distinct behaviors, demonstrating different phases of the Hamiltonian and implying the simulation of dynamical phase transitions.

3. Quantum supremacy and quantum computational advantage

It is interesting to know what kind of computational problem can be solved by both quantum computers and classical computers, and at the same time, the state-of-the-art quantum computers can perform better, even exponentially faster, than the most advanced classical computers. This aim can be named as quantum supremacy[2,17] or quantum computational advantage. It is pointed out that the task of sampling random quantum circuits output can demonstrate the computational capability of a quantum computer while it is a hard problem for classical computers.[18] To achieve the quantum supremacy, a prerequisite condition is that the number of qubits N should be larger than around 50, which corresponds to computational state space of dimension 2^N. Additionally, the depth of the random quantum circuits should be larger than a threshold such that this computation by classical approach will take a long time, for example, hundreds of years. These two conditions may have tradeoff relations.

The random quantum circuits can create a quantum state $|\Psi\rangle = U_{\rm rd}|\vec{0}\rangle$. There are N qubits. So $\vec{0}$ defines that all N qubits are initialized as $|0\rangle$. The sampling of the output $|\Psi\rangle$ will produce a series of bitstrings $\vec{x}_j$ with the form like $0100\cdots$ for N bits. Suppose k times sampling of random but fixed quantum circuits $U_{\rm rd}$ are made, the aim is that the results of the sampling should satisfy the following inequality:

$$\frac{1}{k}\sum_{j=1}^{k}|\langle\vec{x}_j|U_{\rm rd}|\vec{0}\rangle|^2 \geq \frac{b}{D}, \tag{3}$$

where D is the dimension $D = 2^N$, b should be larger than 1, but may not larger than 2.[2]

A quantum state can be written in the superposed form as $|\Psi\rangle = \sum_j p^{\frac{1}{2}}(\vec{x}_j)|\vec{x}_j\rangle$, here the phase parameters have been omitted since they will not affect the results of the sampling. It is assumed that for a random quantum circuit $U_{\rm rd}$, the distribution of the probability $\Pr(p)$ satisfies the Porter–Thomas distribution defined by the form[2] $\Pr(p) = D\,\mathrm{e}^{-Dp}$. It means that the number of bitstrings with amplitude parameter in the region $[p, p+\mathrm{d}p]$ is $D\Pr(p)\mathrm{d}p = D^2\,\mathrm{e}^{-Dp}\mathrm{d}p$.

Now, we suppose that the sampling task can be performed by measuring the state $|\Psi\rangle$ on computational basis, implying that bitstings $\vec{x}_j$ can be obtained with the probability $p(\vec{x}_j)$ corresponding to its amplitude. So, the bitstrings obtained by sampling take the distribution form $f(p) = pD^2\,\mathrm{e}^{-Dp}$. Then, according to the aim of the computational task, we should calculate the circuits defined amplitude $p(\vec{x}_j)$ with the $f(p)$ sampling distribution, resulting in $\int_0^1 pf(p)\mathrm{d}p \approx 2/D$. This result is true only in the case that the sampling can be made perfectly. If there are errors, for example in an extreme condition that the bitstrings are randomly chosen with the identical distribution $1/D$, the obtained quantity will take the form $\int_0^1 \frac{p}{D}\mathrm{d}p \approx \frac{1}{D}$. It is now clear that the sampling random quantum circuits by a quantum computer with noise will give a quantity b which ranges from 1 to 2, corresponding respectively to cases of completely random and perfect sampling. While for a general b, $b \in [1,2]$, it corresponds how well the sampling task is completed.

The problem is that the quantity b is based on the knowledge of the amplitude $p(\vec{x}_j)$ defined by a unitary operator $U_{\rm rd}$, which is realized by a random quantum circuit. The computation of the amplitudes $p(\vec{x}_j)$ generally is a hard problem by classical approaches. For a quantum computer, in order to characterize the performance of the sampling, it is proposed that the linear cross-entropy fidelity, $F_{\rm XEB}$, can be used as a figure of merit. Remarkably, the fidelity $F_{\rm XEB}$ is related with $b = 1 + F_{\rm XEB}$, both quantifies the extent of success in sampling the defined state. So the performance of the sampling depends on the proposed fidelity. For quantum computation, the fidelity $F_{\rm XEB}$ can be reasonably estimated, based on experimental data and numerical results for simpler circuits.[2] The sampling bitstrings are obtained by repeatedly measuring the prepared state $|\Psi\rangle$ realized by a random quantum circuit. The computational task can then be performed. In contrast for a classical computer, it is hard to calculate a series of amplitude $p(\vec{x}_j)$ for bitstring $\vec{x}_j$ since the handling of state dimension D and the calculation of deep circuits $U_{\rm rd}$ are beyond the computational capability of the current computer.

Recently, the quantum supremacy is realized firstly by Google AI quantum team using 53-qubit programmable superconducting quantum processor, named as Sycamore.[2] Later, similar computational tasks are performed with more superconducting qubits[3] or larger dimension of computational state in optics system.[19] For superconducting qubits, the random quantum circuits are composed of single qubit rotation gates, $X^{1/2}, Y^{1/2}, (X+Y)^{1/2}$, and two-qubit entangling gates between nearest neighbor qubits located in a square lattice in the processor. It is pointed out that one million sampling time can be performed for a quantum circuit with about 200 s, while similar computational task will take about 10000 years for a powerful supercomputer.[2] A similar experiment is also presented with more superconducting qubits.[3] It is then shown that a quantum computer outperforms the classical computers for a specific task.

On the other hand, remarkable progresses have been made in sampling random quantum circuits by classical computers, see Refs. [20,21]. In case the competition between quantum computers and classical computers is on going, the study itself has put forward interesting problem to explore the current boundaries for both quantum and classical computations. We are still optimistic about the practical computational capability of quantum computation, which may be beyond the classical computers.

4. Quantum simulation of localization and thermalization

At the present NISQ stage, localization and thermalization can be simulated by various quantum platforms. For an isolated quantum system, an initial quantum state will generally evolve to equilibrium. Although the whole system itself is a pure state, the subsystem behaves like being thermalized with its reduced density matrix taking the form of thermalized states with a temperature. However, at specific conditions such as integrability, on-site or interaction disorders, the system will remain as localized state. Those conditions leading to localized states can be realized in different systems, which are then demonstrated in many recent experiments showing the controllability of the platforms. In principle, these experiments realized different phases of the quantum matter by presenting dynamical properties of the simulated systems. On the other hand, occurring of thermalization in an isolated quantum system itself is an interesting problem and is worth exploring experimentally.

There are different types of localization, such as Anderson localization for non-interacting particles with disorders, and many-body localization (MBL) for interacting systems. MBL has been realized by trapped ions with ten qubits.[22] The system Hamiltonian is an Ising type with long-range interactions, and the disorder is applied by the on-site random potential. The occurring of MBL is predicted by Poisson distribution for level statistics calculated for the system. The MBL is demonstrated in experiment by data of time-evolved local magnetization and dynamics of quantum Fisher information corresponding entanglement.

The MBL is also realized in a two-dimensional optical lattice for a Bose–Hubbard model with controllable on-site disorder. The time-evolved imbalance is used to identify transition of MBL and thermalization.[23]

It is expected that entanglement entropy, which is obtained by using reduced density matrix of the subsystem, will grow logarithmically in terms of time for MBL. In contrast, it will reach quickly to a constant related with the volume law for thermalization because of eigenvector thermalization hypothesis.[24] Experimentally, a density matrix can be obtained by state tomography. However, times of measurement for state tomography will grow exponentially in terms of qubits number, which is a challenge for experiments when the number of qubits is relatively large. By using a 10-qubit superconducting processor with all-to-all connectivity, the MBL is realized with programmable controlled random on-site potentials.[8] The time-evolved reduced density matrix of 5 qubits is obtained by using state tomography. Based on those results, the entanglement entropy logarithmic growth with time is observed, as shown in Fig. 2.

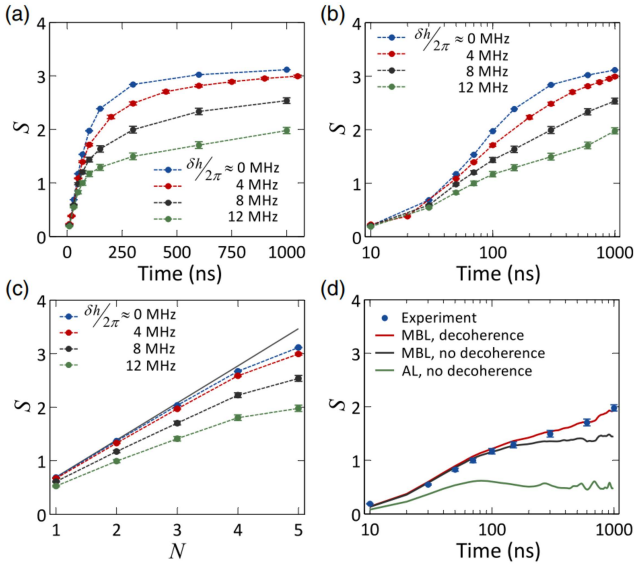


Fig. 2. Half-chain entanglement entropy, which is extracted from the experimentally measured 5-qubit density matrix by performing quantum state tomography. (a), (b) The entanglement entropy S as functions of the evolution time for different disorder strengths δh is plotted in linear scale and in logarithmic scale, respectively, (c) Site-averaged S at around 1000 ns as a function of the qubits number N. (d) The comparison between MBL and Anderson localization. Dots are experimental data, and lines are numerical simulation. Figures are adapted from Ref. [8].

The measurement of density matrix with many qubits by tomography generally is difficult in experiments. Alternatively, the second order Rényi entanglement entropy based on square of the density matrix can be obtained by using randomized measurements, which is performed for 10 qubits for MBL in ion-trap system.[25] At the same time, the second order Rényi entanglement entropy is also obtained, based on particle fluctuations and correlations measuring on up to 10 qubits of trapped ions.[26]

5. Generation of multi-qubit entanglement

Entanglement is a necessary resource for quantum computation.[28–32] Also, preparation of multi-qubit entanglement is a benchmark in showing the control capability of different platforms, in particular for preparing the Greenberger–Horne–Zeilinger (GHZ) type of states.[33] The N-qubit GHZ states take a simple superposed form

$$|\mathrm{GHZ}\rangle_N = \frac{1}{\sqrt{2}}(|00\cdots0\rangle + |11\cdots1\rangle). \tag{4}$$

One interesting property of the multipartite GHZ states is that all particles are globally entangled, while there is no entanglement between particles for a subsystem in case another subsystem is traced off.[33]

Recently, the number of qubits in GHZ-type states preparations can reach 18 and 20, for superconducting qubits[27,34] (see Fig. 3) and Rydberg atoms,[35] respectively. For photons and trapped ions, the number of qubits for GHZ entanglement generation can be 14 by ions,[36] 12 by photons[37] and 18 by using six photons with three degrees of freedom.[38]

Besides simulating many-body physics such as quantum phase transitions by different platforms, on the other hand, we may exploit the quantum phase transitions as a mechanism in entanglement generation. For example, it is reported that many-body entanglement of around 11000 atoms can be deterministically generated in a system of rubidium-87 Bose–Einstein condensate.[39] By simulating dynamical quantum phase transitions, it is shown that multiple qubit can be entangled to generate a spin squeezed state near the dynamical critical point with a 16-qubit superconducting quantum processor.[40] So different methods are worth exploring in preparing various entangled states for tasks of quantum information processing.

We know that entanglement, such as squeezed state, is a resource for quantum metrology with entanglement-enhanced phase sensitivity.[41,42] It is interesting that there is a close relationship between Gaussian squeezed state and entanglement by using squeezing parameter. However, the non-Gaussian entangled states cannot be well characterized by using the standard squeezing parameter, a generalization as nonlinear squeezing parameter[43] should be exploited. Experimentally, it is generally challenging to measure the nonlinear squeezing parameter. Recently, by using a superconducting quantum

processor, the nonlinear squeezing parameter is obtained to characterize a 19-qubit non-Gaussian entangled state, showing quantum-enhanced metrological gain.[44]

On the other hand, we know that entanglement can be used to process quantum computation in a way that may reduce the complexity compared with direct implementation of the computational task, for example in one-way quantum computation.[28] It will be plausible that entanglement may be accessed conveniently for researchers for exploring various quantum computing applications. The online generation of entanglement will then be very useful and can be conveniently exploited for various purposes. Besides, the cloud quantum computation itself is expected as the infrastructure in deploying quantum computation facilities. However, the generation of entanglement generally involves its verification which needs techniques such as repeated measurements with changing parameters. The online generation and verification of entangled states such as GHZ states become a difficult task. Recently, the cloud quantum computation platform, named as ScQ implying superconducting quantum, has been constructed. Based on high efficiency of the operating system of the experimental setup, the GHZ states of up to 10 qubits have been created and also verified by using fidelity which relies on the standard method by measuring both amplitude and parity quantities.[45] By measuring parity, the rotation operation $\otimes_j \exp(\mathrm{i}\frac{\pi}{4}\sigma_\phi^j)$ should be applied collectively on all qubits, and repeated measurements should be performed with changing ϕ ranging for several periods. With those operations, fidelities of all the generated GHZ states have been provided. The results show that our ScQ platform is ranked as one of the best cloud quantum computation platforms.

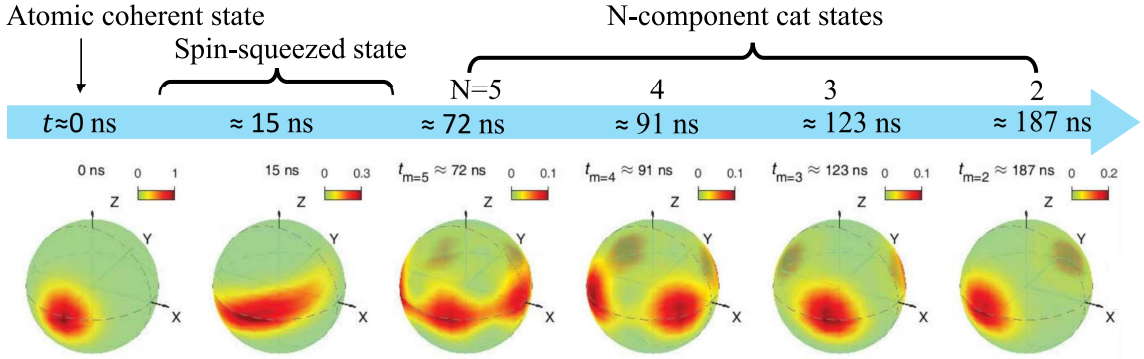


Fig. 3. Multicomponent atomic Schrödinger cat states of 20 qubits. Plotted are the experimentally measured Q-functions at specific time intervals of state evolution under an all-to-all coupled Hamiltonian with up to 20 qubits. The system is firstly initialized in an atomic coherent state, then coherently evolves to the spin-squeezed state and finally to the multicomponent atomic Schrödinger cat states including the GHZ state. The figure is adapted from Ref. [27].

6. Perspectives

In the past years, quantum computation largely demonstrate proof-in-principle results by noisy processors with small and intermediate-scale number of qubits or qudits, meaning higher-dimensional quantum states. To make quantum computing practical, many technical challenges need be overcome to improve the scalability and coherence of qubits. In the long term, we aim to build a fault-tolerant quantum computer which can solve any problem. While in the short term, using noisy quantum processors with more qubits and better performance, we can still apply the quantum computing to some specific practical problems.

The near-term perspectives may need to pay close attention to hybrid processors, which are based on maturely classical processors and developing quantum functional devices. One of the main aims is to find practical applications by using near-term quantum devices assisted by classical processors. The potential applications are based on what we just reviewed, and more applications are worth studying.

The realization of universal quantum computers is challenging, which may depend on the success of quantum error correction. Different methods have been explored, but the full advantages of the quantum error correction are to be realized in the future. The techniques to realize the quantum computers are not yet fixed. The main barriers that need be solved are scalability and high control precision.

It is obvious that the research of quantum computation is one of the main research areas in the past years. More results are still expected to realize and more attention will be attracted to this field.

Acknowledgements

This work is supported in part by the National Natural Science Foundation of China (Grant Nos. 11934018, T2121001, 11904393, and 92065114), the CAS Strategic Priority Research Program (Grant No. XDB28000000), Beijing Natural Science Foundation (Grant No. Z200009), and Scientific Instrument Developing Project of Chinese Academy of Sciences (Grant No. YJKYYQ20200041).

References

[1] Preskill J 2018 *Quantum* **2** 79

[2] Arute F and Arya K, Babbush R, *et al.* 2019 *Nature* **574** 505
[3] Wu Y and Bao W S, Cao S, *et al.* 2021 *Phys. Rev. Lett.* **127** 180501
[4] Bernien H, Schwartz S, Keesling A, Levine H, Omran A, Pichler H, Choi S, Zibrov A, Endres M, Greiner M, Vuletic V and Lukin M 2017 *Nature* **551** 579
[5] Zhang J, Pagano G, Hess P, Kyprianidis A, Becker P, Kaplan H, Gorshkov A, Gong Z X and Monroe C 2017 *Nature* **551** 601
[6] Guo Q, Cheng C, Sun Z H, Song Z, Li H, Wang Z, Ren W, Dong H, Zheng D, Zhang Y R, Mondaini R, Fan H and Wang H 2021 *Nat. Phys.* **17** 234
[7] Guo Q, Cheng C, Li H, Xu S, Zhang P, Wang Z, Song C, Liu W, Ren W, Dong H, Mondaini R and Wang H 2021 *Phys. Rev. Lett.* **127** 240502
[8] Xu K, Chen J J, Zeng Y, Zhang Y R, Song C, Liu W, Guo Q, Zhang P, Xu D, Deng H, Huang K, Wang H, Zhu X, Zheng D and Fan H 2018 *Phys. Rev. Lett.* **120** 050507
[9] Aspuru-Guzik A, Dutoi A D, Love P J and Head-Gordon M 2005 *Science* **309** 1704
[10] Liu J, Lim K H, Wood K, Huang W, Chu G and Huang H L 2021 *Sci. China Phys. Mech. Astron.* **64** 290311
[11] Cong I, Choi S and Lukin M 2019 *Nat. Phys.* **15** 1273
[12] Lloyd S and Weedbrook C 2018 *Phys. Rev. Lett.* **121** 040502
[13] Huang K, Wang Z A, Song C, Xu K, Li H, Wang Z, Guo Q, Song Z, Liu Z B, Zheng D, Deng D L, Wang H, Tian J G and Fan H 2021 *NPJ Quantum Inf.* **7** 165
[14] Feynman R P 1982 *Int. J. Theor. Phys.* **21** 467
[15] Wu X, Liang X, Tian Y, Yang F, Chen C, Liu Y C, Tey M K and You L 2021 *Chin. Phys. B* **30** 020305
[16] Chen W, Gan J, Zhang J N, Matuskevich D and Kim K 2021 *Chin. Phys. B* **30** 060311
[17] Preskill J 2012 arXiv: 1203.5813v3 [quant-ph]
[18] Aaronson S and Arkhipov A 2010 *Proceedings of the Annual ACM Symposium on Theory of Computing* **9** 333
[19] Zhong H S and Wang H, Deng Y H, *et al.* 2020 *Science* **370** 1460
[20] Pan F and Zhang P 2022 *Phys. Rev. Lett.* **128** 030501
[21] Pan F, Chen K and Zhang P 2021 arXiv: 2111.03011v1 [quant-ph]
[22] Smith J, Lee A, Richerme P, Neyenhuis B, Hess P, Hauke P, Heyl M, Huse D and Monroe C 2016 *Nat. Phys.* **12** 907
[23] Choi J Y, Hild S, Zeiher J, Schauß P, Rubio-Abadal A, Yefsah T, Khemani V, Huse D A, Bloch I and Gross C 2016 *Science* **352** 1547
[24] Nandkishore R and Huse D A 2015 *Annu. Rev. Condens.* **6** 15
[25] Brydges T, Elben A, Jurcevic P, Vermersch B, Maier C, Lanyon B P, Zoller P, Blatt R and Roos C F 2019 *Science* **364** 260
[26] Lukin A, Rispoli M, Schittko R, Tai M E, Kaufman A M, Choi S, Khemani V, Léonard J and Greiner M 2019 *Science* **364** 256
[27] Song C, Xu K, Li H, Zhang Y R, Zhang X, Liu W, Guo Q, Wang Z, Ren W, Hao J, Feng H, Fan H, Zheng D, Wang D W, Wang H and Zhu S Y 2019 *Science* **365** 574
[28] Raussendorf R and Briegel H J 2001 *Phys. Rev. Lett.* **86** 5188
[29] Huang H L, Wu D, Fan D and Zhu X 2020 *Sci. China Inf. Sci.* **63** 180501
[30] Hao S, Deng X, Liu Y, Su X, Xie C and Peng K 2021 *Chin. Phys. B* **30** 060312
[31] He K, Geng X, Huang R, Liu J and Chen W 2021 *Chin. Phys. B* **30** 080304
[32] Song C, Xu K, Liu W, Yang C P, Zheng S B, Deng H, Xie Q, Huang K, Guo Q, Zhang L, Zhang P, Xu D, Zheng D, Zhu X, Wang H, Chen Y A, Lu C Y, Han S and Pan J W 2017 *Phys. Rev. Lett.* **119** 180511
[33] Gühne O and Tóth G 2009 *Phys. Rep.* **474** 1
[34] Wei K X, Lauer I, Srinivasan S, Sundaresan N, McClure D T, Toyli D, McKay D C, Gambetta J M and Sheldon S 2020 *Phys. Rev. A* **101** 032343
[35] Omran A, Levine H, Keesling A, Semeghini G, Wang T T, Ebadi S, Bernien H, Zibrov A S, Pichler H, Choi S, Cui J, Rossignolo M, Rembold P, Montangero S, Calarco T, Endres M, Greiner M, Vuletić V and Lukin M D 2019 *Science* **365** 570
[36] Monz T, Schindler P, Barreiro J T, Chwalla M, Nigg D, Coish W A, Harlander M, Hänsel W, Hennrich M and Blatt R 2011 *Phys. Rev. Lett.* **106** 130506
[37] Zhong H S, Li Y, Li W, Peng L C, Su Z E, Hu Y, He Y M, Ding X, Zhang W, Li H, Zhang L, Wang Z, You L, Wang X L, Jiang X, Li L, Chen Y A, Liu N L, Lu C Y and Pan J W 2018 *Phys. Rev. Lett.* **121** 250505
[38] Wang X L, Luo Y H, Huang H L, Chen M C, Su Z E, Liu C, Chen C, Li W, Fang Y Q, Jiang X, Zhang J, Li L, Liu N L, Lu C Y and Pan J W 2018 *Phys. Rev. Lett.* **120** 260502
[39] Luo X Y, Zou Y Q, Wu L N, Liu Q, Han M F, Tey M K and You L 2017 *Science* **355** 620
[40] Xu K, Sun Z H, Liu W, Zhang Y R, Li H, Dong H, Ren W, Zhang P, Nori F, Zheng D, Fan H and Wang H 2020 *Sci. Adv.* **6** eaba4935
[41] Giovannetti V, Lloyd S and Maccone L 2011 *Nat. Photon.* **5** 222
[42] Caves C M 1981 *Phys. Rev. D* **23** 1693
[43] Gessner M, Smerzi A and Pezzè L 2019 *Phys. Rev. Lett.* **122** 090503
[44] Xu K, Zhang Y R, Sun Z H, Li H, Song P, Xiang Z, Huang K, Li H, Shi Y H, Chen C T, Song X, Zheng D, Nori F, Wang H and Fan H 2022 *Phys. Rev. Lett.* **128** 150501
[45] Chen C T, Shi Y H, Xiang Z C, Wang Z A, Li T M, Sun H Y, He T S, Song X H, Zhao S P, Zheng D, Xu K and Fan H 2022 arXiv: 2203.03000v1 [quant-ph]